Water Vapor Transport Associated with the Summertime North American Monsoon as Depicted by ECMWF Analyses

JEFFREY T. SCHMITZ* AND STEVEN L. MULLEN

Department of Atmospheric Sciences, The University of Arizona, Tucson, Arizona

(Manuscript received 6 April 1995, in final form 11 January 1996)

ABSTRACT

The origins and transport of water vapor into the semi-arid Sonoran Desert region of southwestern North America are examined for the July–August wet season. Vertically integrated fluxes and flux divergences of water vapor are computed for the 8 summers 1985–1992 from ECMWF mandatory level analyses possessing a spectral resolution of triangular 106 (T106).

The ECMWF analyses indicate that transports of water vapor by the time-mean flow dominate the transports by the transient eddies. Most of the moisture at upper levels (above 700 mb) over the Sonoran Desert arrives from over the Gulf of Mexico, while most moisture at low levels (below 700 mb) comes from the northern Gulf of California. There is no indication of moisture entering the Sonoran Desert at low levels directly from the southern Gulf of California or the tropical East Pacific. Water vapor from the tropical East Pacific can enter the region at upper levels after upward transport from low levels along the western slopes of the Sierra Madre Occidental of Mexico and subsequent horizontal transport aloft.

The T106 ECMWF analyses, when only the mandatory level analyses are used, do not possess sufficient resolution to yield accurate estimates of highly differentiated quantities such as the divergence of the vertically integrated flux of water vapor. Even at a T106 resolution, the northern Gulf of California and the terrain of the Baja California peninsula are not adequately resolved.

1. Introduction

As the boreal solstice approaches, the North Pacific High builds off the west coast of North America, relinquishing much of its influence on the Sonoran Desert region of the SW United States and NW Mexico. (Figure 1 shows a map with the geographical regions referred to in this paper.) Simultaneously, the Bermuda high thrusts northwestward into the region, and the time-mean midtropospheric (500–700 mb) flow backs from WNW during May and June to SSE during July and August. Concurrent with the wind shift, precipitable water and convective activity over the region increase dramatically. Consideration of the change in the prevailing wind and the geographical distribution of land–sea boundaries led many earlier researchers (Reed 1993; Jurwitz 1953; Bryson and Lowry 1955; Reitan 1957) to conclude that the summertime moisture over the Sonoran Desert is transported from the Gulf of Mexico, along the western flank of the Bermuda High.

An analysis of the water vapor transport over North America by Benton and Estoque (1954), however, suggested another source of summertime moisture situated to the west of the Continental Divide, separate from the larger flux from the Gulf of Mexico. More evidence of a Pacific source of moisture came from Rasmusson (1967), whose analysis showed that water vapor east of the divide clearly originates from the Gulf of Mexico/Caribbean Sea, while moisture over the Sonoran Desert appears to originate from the Gulf of California. The issue of moisture from the tropical East Pacific was not resolved because neither analysis extended into Mexico.

Hales (1972, 1974) proposed that moisture over the Sonoran Desert comes in the form of short-lived, low-level surges up the Gulf of California. Brenner (1974) concurred, adding that these surges appear to be independent from the large-scale circulation. Both Hales and Brenner expressed skepticism that moisture from the Gulf of Mexico could pass over the Sierra Madre Occidental range and still make significant contributions to the precipitable water over the Sonoran Desert. Sellers and Hill (1974), on the other hand, maintained that monsoon moisture comes primarily from the Gulf of Mexico.

* Current affiliation: Starburst Technologies, LTD, Scottsdale, Arizona.

Corresponding author address: Steven L. Mullen, Department of Atmospheric Sciences, PAS Building #81, The University of Arizona, Tucson, Arizona 85721.
E-mail: mullen@air.atmo.arizona.edu

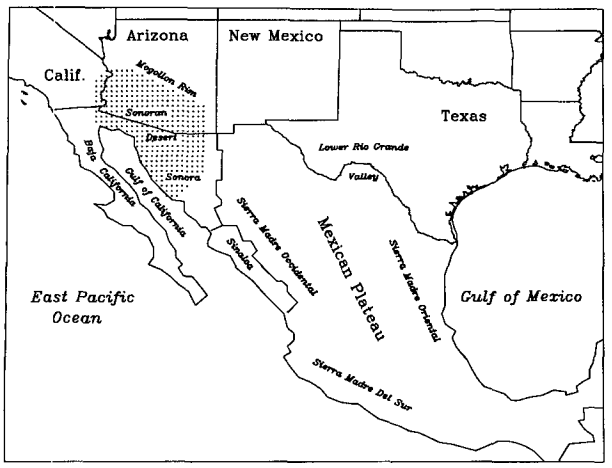

FIG. 1. Geography of the SW North American region showing locations mentioned in the text. Stipled region indicates portion of the Sonoran Desert emphasized in this analysis. We have excluded that portion over the Baja peninsula. The greater Sonoran Desert, or Desert Southwest will be used to refer to the broader region surrounding the Sonoran Desert.

Reyes and Cadet (1986, 1988) examined moisture flux over the tropical Americas during the period May–August 1979. They proposed that the intensification of the South Pacific anticyclonic gyre propels low-level moisture across the equator toward western Mexico. Once there, it could reach the Sonoran Desert either at low levels as a result of southeasterly gulf surges or at midlevels after convective mixing with midtropospheric moisture from the east and subsequent transport northward around the western flank of the subtropical ridge. Their description stressed the importance of both Gulf of Mexico and tropical East Pacific moisture sources and the coupling of the two through convective transport.

Recent research using data from special field programs provides further evidence for a low-level flux of water vapor along the Gulf of California (Badan-Dangon et al. 1991; Douglas et al. 1993). Contrary to the short-lived surges proposed by Hales (1972, 1974) and Brenner (1974), these studies reveal a persistent transport of moisture along the Gulf of California by the time-mean wind. Douglas et al. (1993) also show that relatively dry air at midlevels is advected from east of the Sierra Madre Occidental toward western Mexico, and they argue that most of the moisture over the Sonoran Desert comes from the tropical East Pacific Ocean or directly off the Gulf of California.

To this day, two fundamental issues remain unresolved: 1) the relative importance of the Gulf of Mexico, the Gulf of California, and the eastern tropical Pacific as moisture sources for the Sonoran Desert, and 2) the primary means by which the moisture is transported into the region. The issues are of more than academic interest, they also have operational implications if seasonal precipitation forecasts for the region during the summer are ever to be realized. Hence, we believe that the need exists to examine these issues further.

To provide insight into these questions, this paper presents results from a diagnosis the moisture flux and water vapor balance over SW North America and adjacent ocean environs for the July–August period using a multiyear, high-resolution dataset produced by a modern-day atmospheric forecast/analysis system. Although the Desert Southwest has been included in many prior investigations of the transport and balance of water vapor, most were based on only a single month, season, or year of data (Benton and Estoque 1954; Starr and Peixoto 1958; Starr et al. 1965; Reyes and Cadet 1988; Trenberth 1991). The question of representativeness arises in view of the intraseasonal and interannual variability that characterizes the region (Carleton 1985, 1986; Carleton et al. 1990). A few multiyear climatologies that included SW North America exist, but these often concerned themselves with differences among the annual means (e.g., Rosen et al. 1979). Even when winter and summer regimes were explicitly contrasted, conditions for June, July, and August are usually averaged to represent the summer mean (Oort 1983; Peixoto and Oort 1992; Roads et al. 1994). Because June conditions are so drastically different from those of July and August (Douglas et al. 1993), its inclusion would distort the flow patterns of "wet" phase of the monsoon. Moreover, all of these studies relied either on radiosonde data that effectively ignores the adjacent oceanic regions, or on gridded datasets having resolutions much too coarse to resolve the Gulf of California, a postulated source of moisture for the Sonoran Desert.

As a means to address the problem using modern-day atmospheric analyses possessing finer spatial and higher temporal resolutions than in previous studies, this work utilizes the global analyses from the European Centre for Medium-Range Weather Forecasts (ECMWF) to compute an 8-year climatology of the water vapor flux and balance associated with the summer phase of the North American Monsoon. No such analysis *focusing on the semi-arid Sonoran Desert* has been done using ECMWF analyses.

This paper is organized as follows. Sections 2 and 3 describe the ECMWF analyses and the methodology, respectively. Section 4 provides a brief overview of the climatology for the region of interest. Results for the transport of water vapor and its flux divergence are presented in section 5. Conclusions and future research directions are discussed in section 6.

2. Data

Uninitialized global analyses produced by the ECMWF are used in this study. The analyses were obtained from the National Center for Atmospheric Research (NCAR). Analyses are available four times

daily (0000, 0600, 1200, and 1800 UTC) for the surface and 14 mandatory levels from 1000 to 10 mb (the recently added 925-mb level is not included). The spectral truncation for the ECMWF analyses is triangular 106 (T106). Analyses at ECMWF are now performed at T213, but these were not contained in the NCAR archives at the time of this study.

The spectral coefficients for all available analyses for the period July and August, 1985–1992, are first transformed to a Gaussian grid having a spacing of approximately 1.125° lat × 1.125° long. To limit the data storage requirements and allow for processing on local workstations, only a subset of the globe covering the region of interest, bounded approximately (to the nearest five degrees) by 5°–50°N, 75°–130°W inclusive was transferred to The University of Arizona for analysis. Since virtually all of the water vapor in the atmosphere occurs below 200 mb, only analyses for the surface and eight lowest mandatory levels (1000, 850, 700, 500, 400, 300, 250, 200 mb) are included in the calculation.

Because the ECMWF analyses are operational, they undergo continuous changes in the data analysis procedures. These changes can produce temporal trends and discontinuities that could impact long-term climatic means and eddy statistics (e.g., Trenberth and Olson 1988). Moreover, the divergent wind component, vertical velocity, and moisture, the three crucial quantities required to compute an accurate moisture budget, are the fields most adversely affected (Trenberth and Olson 1988). Furthermore, over data sparse regions, such as the oceans and to a lesser degree over Mexico itself, analysis quantities are largely determined by the first-guess forecast fields even at the synoptic hours of 0000 UTC and 1200 UTC. Clearly the validity of any conclusions drawn using the ECMWF analyses depends critically on their integrity.

While it is very difficult, if not impossible, to determine precisely the fidelity of the ECMWF analyses, estimates of the uncertainty can be obtained. The uncertainty in the derived water vapor budgets and moisture fluxes can be estimated assuming the wind and specific humidity at each grid point have an accuracy comparable to radiosonde data. This clearly denotes a lower bound estimate of the uncertainty. Thus, whenever a budget value is less than that due to the analysis uncertainty, the budget value must be considered insignificant. A crude consistency check can also be made by comparing our results for the T106 ECMWF analyses to previous results based solely on the analysis of radiosonde data.

3. Analysis procedures

a. *Vertically integrated, atmospheric flux of water vapor*

To illustrate the water vapor transport for the monsoonal period, vertically integrated moisture flux vectors ($\mathbf{Q}$) can be computed:

$$\mathbf{Q} = \int_{p_{\text{top}}}^{p_{\text{sfc}}} (q\mathbf{V}) \frac{dp}{g}, \tag{1}$$

where q is specific humidity, $\mathbf{V}$ is the horizontal wind vector, p_{sfc} is the surface pressure, and p_{top} is the pressure at the top of the atmosphere. It is also of interest to compare the transport at low levels to that at higher levels. To examine this, the moisture flux for the atmospheric layers above and below 700 mb, and the exchange of water mass between them, are considered. In this case, transport vectors are computed by integrating (1) from the surface to 700 mb and from 700 to 200 mb, respectively. The exchange of moisture between these two layers is represented by the vertical flux through the 700-mb level.

b. *Atmospheric water vapor balance*

The general balance equation for atmospheric water vapor can be expressed as

$$E - P = \frac{\partial W}{\partial t} + \nabla \cdot \mathbf{Q} - \frac{\omega_{\text{top}} q_{\text{top}}}{g}, \tag{2}$$

where ω is the pressure vertical velocity, E is evaporation per unit area, P is precipitation per unit area, and W is the precipitable water defined by

$$W = \int_{p_{\text{top}}}^{p_{\text{sfc}}} q \frac{dp}{g}. \tag{3}$$

All other symbols have their usual meteorological meaning. A complete derivation of the general water vapor balance equation is given in the appendix. Equation (2) states that the difference between evaporation and precipitation at the earth's surface equals the sum of the local change in precipitable water, the divergence of the vertically integrated horizontal water vapor flux, and the vertical water vapor transport through the top of the atmosphere. The last term of Eq. (2) is negligible since $q \approx 0$ at 200 mb.

Averaging (2) over time yields

$$\nabla \cdot \mathbf{Q} \approx \bar{E} - \bar{P}, \tag{4}$$

where an overbar denotes a time average over the period July–August. The storage term can be neglected for an averaging period of two months since it is typically much smaller than the mean flux divergence (Starr and Peixoto 1958; Rasmusson 1966; Palmén 1967; Peixoto 1973). Equation (4) also neglects horizontal diffusion and the horizontal transport of liquid and solid phases. Although these are important elements of the water balance for individual convective elements, they are both generally much smaller than the remaining terms when considering long averaging periods such as a month or more, and/or large spatial extents (Starr and Peixoto 1958; Palmén 1963; Peixoto 1973; Rasmusson 1968, 1977) such as a 1.125° × 1.125° grid.

Equation (4) provides an estimate of the mean water balance for a column of air extending from the surface to the top of the atmosphere, or 200 mb in this case. Areas with an excess of evaporation over precipitation ($E - P > 0$) are termed water vapor source regions, while areas with an excess of precipitation over evaporation ($E - P < 0$) are termed sink regions.

c. *Regional balance of water vapor and moisture transport across regional boundaries*

Spatially averaged water vapor budgets can be obtained by integrating (4) over an area A giving

$$\frac{1}{A}\int\int_A \nabla\cdot\mathbf{Q}dA = \{\bar{E} - \bar{P}\},$$

which, with the aid of Gauss' theorem, can be written as

$$\oint_C \mathbf{Q}\cdot\mathbf{n}dC = \{\bar{E} - \bar{P}\}, \qquad (5)$$

where { } denotes an areal average, $\mathbf{n}$ is the outward unit vector normal to the regional boundary, $\mathbf{Q}\cdot\mathbf{n}$ is the moisture transport across the regional boundary, and the line integral is computed along the closed path delimiting the region.

d. *Miscellaneous numerical procedures*

Vertical integrals are calculated by the trapezoid rule, with all fields assumed to vary linearly with pressure between mandatory levels. Spatial derivatives are computed using centered finite differences on the 1.125° grid. This procedure is not consistent with the ECMWF formulation, which operates on the spectral coefficients to obtain horizontal derivatives. Since only a subset of the hemisphere was obtained, we are unable to use spectral processing. As will become clear later, the numerical error introduced by this procedure is negligible compared to other uncertainties and error sources inherent in our analysis.

Time-mean quantities are obtained by averaging over all eight summers and all four analysis times (0000, 0600, 1200, and 1800 UTC). Transient eddy statistics are obtained as departures from the 8-yr seasonal means at the four daily analysis times, then averaging those results over all four analysis times. Thus, interannual variations are contained in the eddy statistics, but contributions from diurnal cycle are excluded. The seasonal cycle is not removed from the data.

4. Overview of the regional climatology for July–August

In this section, the mean July–August wind and moisture fields over SW North American as depicted by the T106 ECMWF analyses are briefly described and compared with results from earlier studies based on other data sources and years. Our primary purpose is not to present a detailed discussion of the regional climate; such information can be found elsewhere (e.g., Douglas et al. 1993). Rather, we desire to provide a proper background in which to interpret the moisture fluxes and budgets and to demonstrate the fidelity of ECMWF analyses.

The large-scale, low-level flow over the region is strongly influenced by the Pacific and Atlantic Subtropical Highs (Fig. 2a), with brisk southerlies over Texas and northwesterlies west of Baja California. Evidence of the thermal low can be seen in the cyclonic winds over the Arizona–California border region. The winds at 500 mb (Fig. 2b) are characterized by easterlies over the Tropics and an anticyclonic circulation centered over southern New Mexico. The upper-level ECMWF winds agree closely with prior analysis of time-mean radiosonde data (e.g., Douglas et al. 1993). The surface and low-level ECMWF winds are also consistent except over the northern Gulf of California, and even in that region the ECMWF analyses denote an improvement over other global objective analyses. Analysis of special field observations (Badan-Dangon et al. 1991; Douglas et al. 1993) reveals that light southerlies to south-southeasterlies mark the time-mean, low-level wind field over the Gulf of California. NMC analyses, for example, place low-level northwesterlies winds over the region (Stensrud et al. 1995). The ECMWF analyses, while not totally consistent with the special field observations, do at least yield a southerly component over the region. The reasons for the erroneous wind directions in the analyses are not known, but as we later discuss it may be a ramification of a horizontal resolution that is still too coarse to adequately resolve the Gulf of California and the surrounding terrain.

A major advantage with using modern objective analyses is that the vertical motion fields, consistent with the model formulations and data assimilation procedures, are available. The time-mean, vertical velocity field at 500 mb (Fig. 3) indicates localized ascent over the southern Rockies and the Sierra Madre Occidental with weaker, more widespread descent situated over the southern Central Plains States, the East Pacific Ocean, and the Gulf of California. The region of upward motion is consistent with precipitation (Douglas et al. 1993; Negri et al. 1994) and infrared cloud climatologies (Douglas et al. 1993), while the overall distribution of vertical velocity is in qualitative agreement with the June, July, and August mean determined by Oort (1983). The ascent over the Sierra Madre Occidental in the ECMWF analyses is much stronger than that given by Oort (1983), however.

The distribution of specific humidity at the surface (Fig. 2b) strongly reflects the underlying terrain, with high values flanking the southern Rockies and the Mexican Plateau. Surface humidity increases eastward into the central United States, and a moist tongue is evident

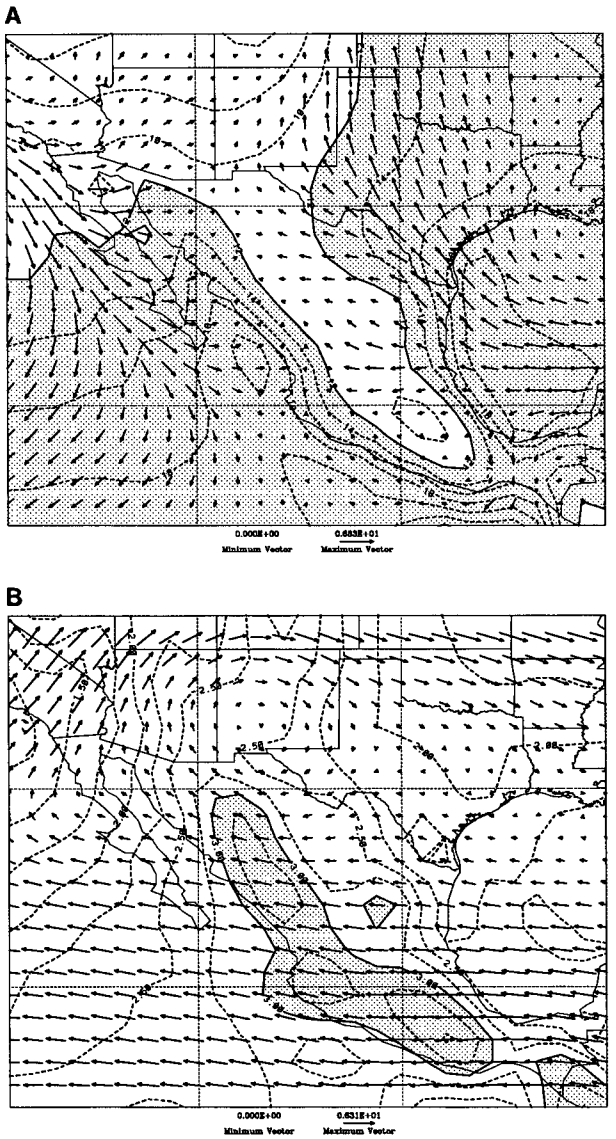

FIG. 2. Time-mean winds and specific humidities for July–August at (a) the surface and (b) 500 mb. Maximum wind vector is 6.8 m s^{-1} and contour interval for q is 2 g kg^{-1} in (a). Maximum wind vector is 6.3 m s^{-1} and contour interval for q is 0.25 g kg^{-1} in (b). Specific humidities $\geq$ 12 g kg^{-1}, and 3 g kg^{-1} are stippled in (a) and (b), respectively. Vector scaling is the same for both panels. For sake of clarity, the boundaries for all figures have been cropped at 15°N, 39°N, 90°W, and 120°W.

over the Gulf of California and the coast of western Mexico. In the middle troposphere (Fig. 2a), a band of enhanced moisture extends northward from the tropical East Pacific into southern Mexico before curving anticyclonically into Arizona and New Mexico. The 500-mb wind and moisture fields indicate that the easterly winds over the Gulf of Mexico advect drier air into western Mexico as discussed earlier by Douglas et al. (1993). The precipitable water (Fig. 4) indicates that deep moisture exists over western Mexico and the tropical East Pacific, with values being larger over that region than anywhere else in the domain. Similar moisture distributions have been previously reported (Starr et al. 1965; Hales 1974; Hagemeyer 1991; Douglas et al. 1993; Negri et al. 1994).

In summary, the mean distributions of the ECMWF wind, vertical velocity, and moisture are qualitatively consistent with results from prior studies. With the noted exception of surface winds over the northern Gulf of California, the T106 ECMWF analyses also appear to give quantitatively accurate, time-mean fields over the domain.

5. Results

a. Vertically integrated, atmospheric flux of water vapor

The distribution of mean flux vectors of water vapor, integrated from the surface to 200 mb (SFC–200 mb), exhibits several noteworthy features over the SW United States and NW Mexico (Fig. 5). On the whole, the SFC–200-mb flux vectors bare close resemblance to the surface wind field (cf. Figs. 5 and 2b), a result that reflects the much larger specific humidities at low levels. Also as expected, the SFC–200-mb flux vectors over the Mexican Plateau are noticeably smaller than neighboring regions, which reflects the impact of underlying high terrain on reducing the limits of the vertical integration.

The strongest flux vectors curve anticyclonically from the Gulf of Mexico into the south-central Plains. A weaker southerly transport is also apparent over the northern Gulf of California and western Arizona. These two moisture streams were first described by Rasmusson (1967). A third feature of interest is a southeasterly

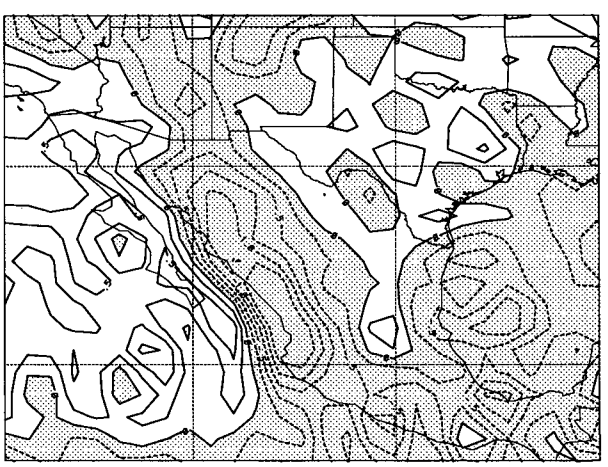

FIG. 3. Time-mean vertical velocity for July–August at 500 mb. Contour interval is 0.25 μb s^{-1}. Stippling indicates upward motion. Vertical velocities $\leq$ 0.25 μb s^{-1} are stippled.

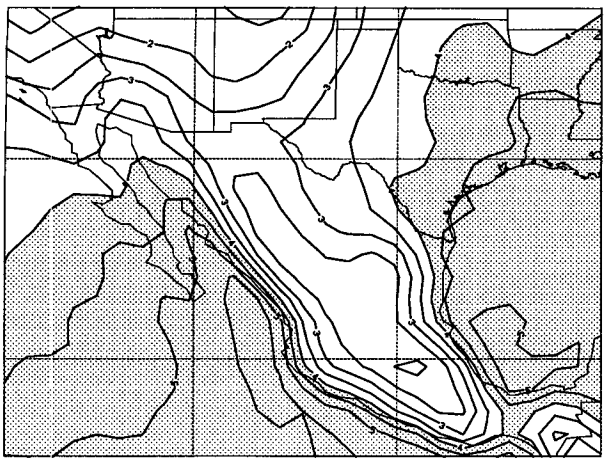

FIG. 4. Time-mean precipitable water (PW) for July–August. Contour interval is 0.5 g cm^{-2}. PW $\geq$ 4 g cm^{-2} is stippled.

flux off the southwest coast of Mexico that emanates from the tropical East Pacific. This moisture plume from the tropical East Pacific, unlike the two described by Rasmusson (1967), appears to flow no farther north than ~25°N, as the flux vectors veer to the west over the southern Gulf of California. Based solely on the distribution of the time-mean SFC–200-mb fluxes, it appears that moisture over the Sonoran Desert comes predominately from the Gulf of Mexico and northern Gulf of California, with little or no input from the tropical East Pacific.

A comparison of the time-mean flow and transient eddy contributions to the moisture transport (Figs. 6a and 6b, respectively) reveals a dominance by the time-mean circulation. While the net transport by the transients is minor compared to that by the time-mean flow, it would be premature to conclude that transient fluctuations are unimportant to the regional water vapor balance. As Roads et al. (1994) point out, it is the instantaneous distribution of the moisture transport that dictates whether precipitation occurs. Moreover, summertime rainfall over the Sonoran Desert shows considerable temporal variability (Bryson and Lowry 1955; Carleton 1986; Watson et al. 1994), a clear in-

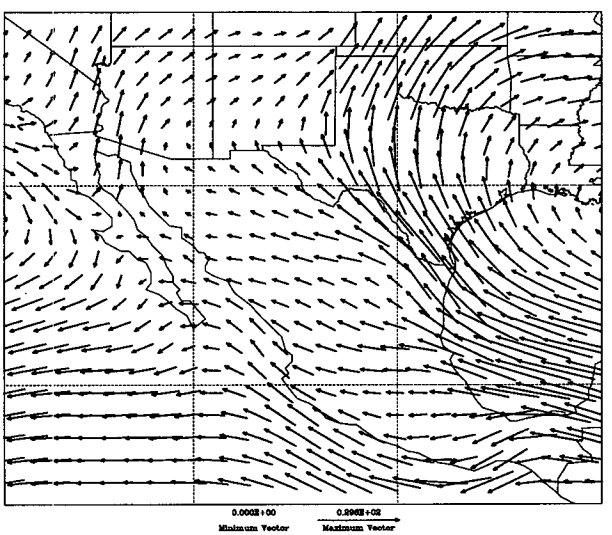

FIG. 5. July–August, total vector flux of water vapor for the surface to 200-mb layer. Maximum vector is 29.6 × 10^2 g cm^{-1} s^{-1}.

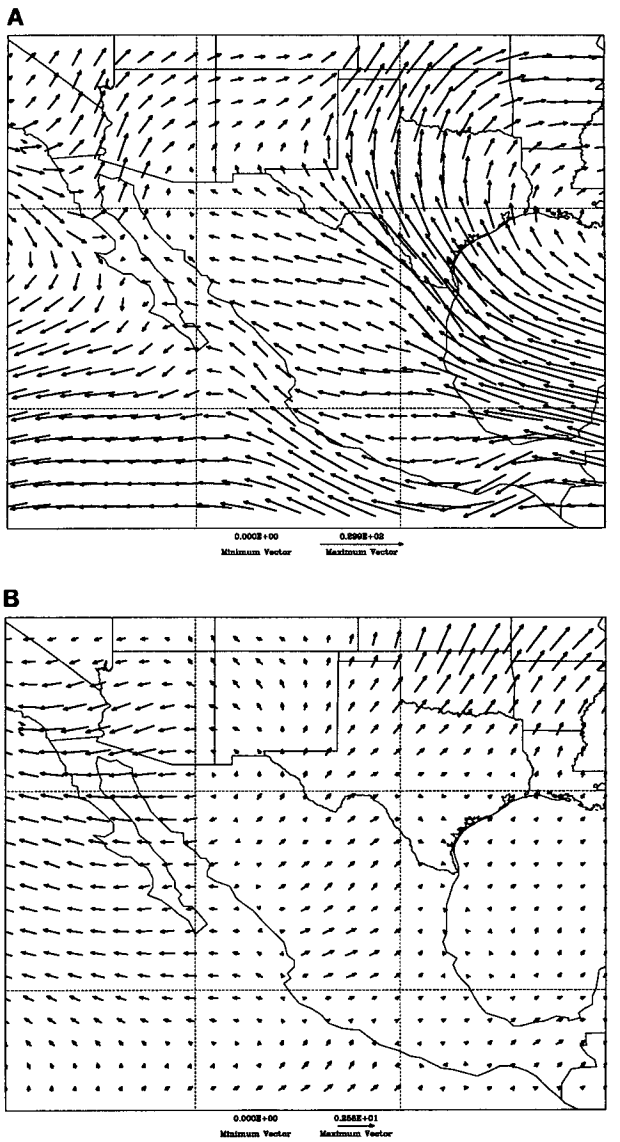

FIG. 6. July–August, vector flux of water vapor due to the time-mean wind for the surface to 200-mb layer due to (a) the time-mean flow and (b) the transient eddies. Maximum vector is 29.9 × 10^2 g cm^{-1} s^{-1} in (a). Vectors in (a) are scaled the same as those in Fig. 5. Maximum vector is 2.6 × 10^2 g cm^{-1} s^{-1} in (b). Vectors in (b) are magnified by a factor of 5 for visual clarity.

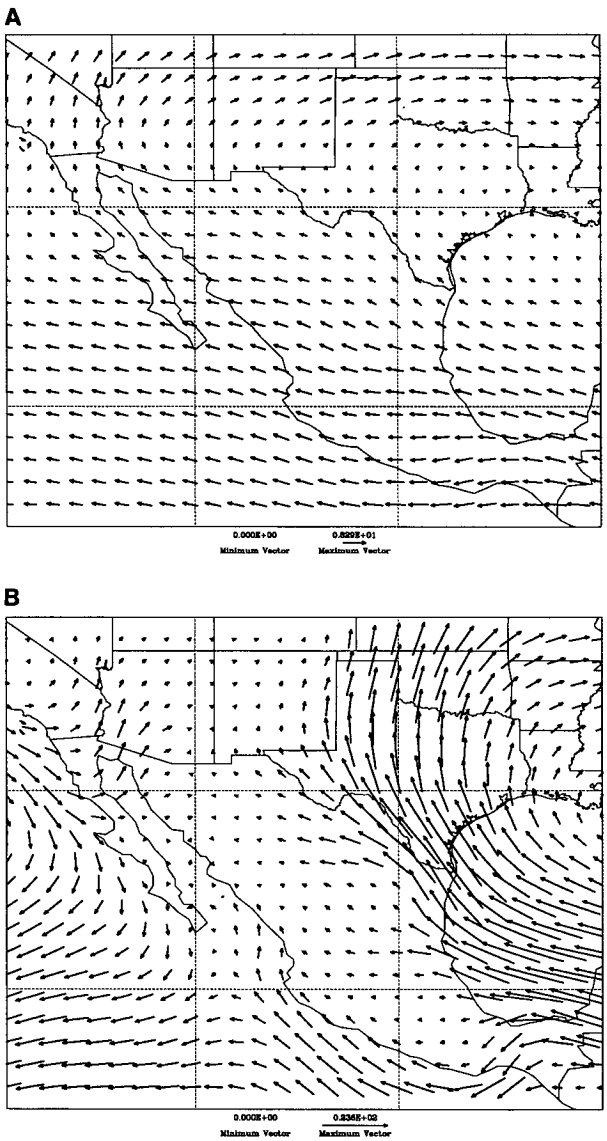

FIG. 7. July–August, total vector flux of water vapor for (a) the 700–200-mb layer and (b) for the surface to 700-mb layer. Vectors in (a) and (b) are scaled the same as those in Figs. 5 and 6a. Maximum vector is 8.3×10^2 g cm^{-1} s^{-1} in (a). Maximum vector is 23.6×10^2 g cm^{-1} s^{-1} in (b).

dication of the importance of transience in modulating precipitation.

The distribution of the transient flux exhibits a pattern that may be related to the underlying orography. The flux vectors fan out from the Sierra Madre Occidental, indicating a transport of moisture away from the mountains. This pattern of divergent vectors appears in every season, suggesting an *intraseasonal* oscillation that is geographically fixed to the mountains and dominates the transient moisture transport. The transport away from mountains may also be related to the strength of the convection along the Sierra Madre Occidental.

While the flux for the SFC–200-mb column depicts the total horizontal transport of water vapor, further insight is offered by examining the flux components above 700 mb (700–200 mb) and below 700 mb (SFC–700 mb) in conjunction with the vertical flux between the two layers. The flux above 700 mb (Fig. 7a) can be characterized as a large-scale rotation about the subtropical high, yielding easterly transport over the Tropics and west Mexico and southerly transport over Arizona. The upper-level moisture over the Sonoran Desert appears to come primarily from above the Gulf of Mexico. Examination of the mean vertical flux through the 700-mb level (Fig. 8), however, indicates a major injection of moisture into the 700–200-mb layer over the Sierra Madre Occidental and the Mogollon Rim of Arizona. The band of strong upward flux coincides with the region of maximum July–August rainfall and undoubtedly reflects the persistent convection that occurs along the mountains during the summer (Douglas et al. 1993; Negri et al. 1994; Watson et al. 1994). A more gradual and widespread downward transport flanks the band of strong upward transport.

The moisture flux in the SFC–700 mb layer (Fig. 7b) is not as simply characterized as that aloft. The dominant signature is the strong flux from the western Gulf of Mexico into Texas. Maximum flux vectors in the region are two to three times larger than maxima elsewhere in the figure. Flux vectors over the Mexican Plateau are generally easterly but small; this indicates little transport of moisture across the continent at low levels. Southwest Arizona and NW Sonora display a strong onshore transport of moisture at low levels from the northern Gulf of California. The flux remains onshore along the entire coastline of Sonora, but is much

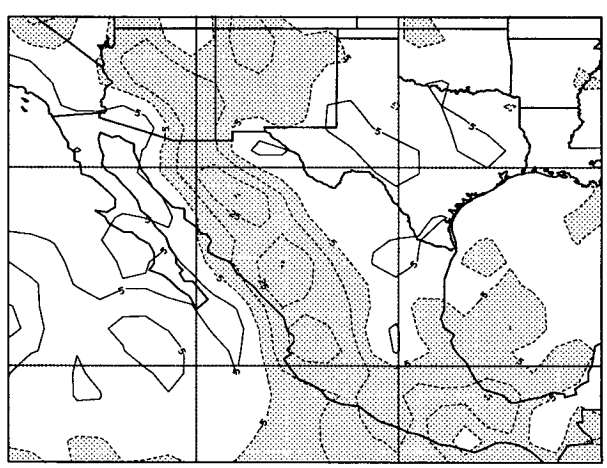

FIG. 8. July–August, total vertical flux of water vapor through the 700-mb layer. Contours are every ±5, ±15, ±25, ... g cm^{-2} month^{-1}; stippling denotes upward flux, solid contours denote downward flux.

stronger to the north. The ECMWF analyses also suggest a noticeable low-level transport across the mountains of northern Baja California from the extratropical East Pacific Ocean into the northern Gulf of California. Another region of noteworthy onshore flux is into Sinaloa, Mexico, where the eastern portion of a southerly stream of moisture from the tropical East Pacific terminates. Over the central Gulf of California, the flux vectors are small. Thus, the ECMWF analyses display little evidence of a time-mean transport of moisture at low levels from the tropical Pacific into the Sonoran Desert.

Although there is little evidence of the mean flow transporting moisture into the Desert Southwest from the tropical East Pacific at low levels, consideration of the vertical flux and the 700–200-mb horizontal transports indicates that moisture from the tropical East Pacific might reach the region aloft. The upward flux over Sinaloa (Fig. 8) would inject East Pacific moisture into the upper atmosphere where it would then cross the Gulf of California and turn northward over the Baja Peninsula. This path would carry the moisture over extreme NW Sonora.

The general features indicated by the horizontal and vertical transports qualitatively agree with the previous findings (e.g., Reyes and Cadet 1988; Roads et al. 1994). Quantitatively, the magnitudes of all fluxes are approximately one order of magnitude larger than our lower-bound estimate of analysis uncertainty assuming gridpoint accuracies comparable to radiosonde observations.

b. Atmospheric balance of water vapor

The time-averaged balance Eq. (4) for water vapor indicates that only the divergence component of the vapor flux contributes directly to the hydrological cycle. It is difficult to infer from the horizontal flux vectors the source and sink regions of water vapor because the rotational component dominates the divergent component in many areas. This situation is clearly the case for Figs. 5 and 6a, both of which are marked by large-scale, anticyclonic curvature about the subtropical highs. For this reason, the distribution of the flux divergence of vertically integrated water vapor was calculated.

The flux divergence for the SFC–200 mb layer (Fig. 9) reveals that, on average, sink regions are situated over the land and source regions are over the adjacent oceans. The regional distribution of sources and sinks, however, is rather complex. The largest values of convergence are situated along the western slopes of the Sierra Madre Occidental where P exceeds E by as much as 35–40 cm mo^{-1}. The band of convergence extends northward along the Mogollon Rim of Arizona and southward into the tropical East Pacific. Its position coincides closely with observed precipitation maxima, and the residual P values (neglecting E over the land,

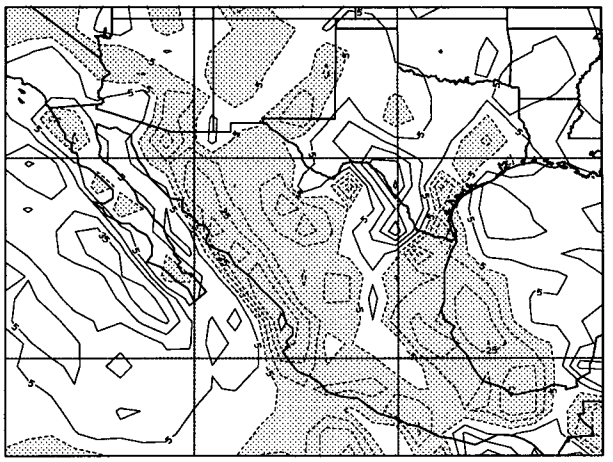

FIG. 9. July–August, flux divergence of the total water vapor transport for the surface to 200-mb layer. Contours are every ±5, ±15, ±25, . . . g cm^{-2} mo^{-1}; stippling denotes convergence, solid contours denote divergence.

a crude assumption) are consistent with, but slightly greater than, the July–August monthly means for the region (Douglas et al. 1993; Negri et al. 1994). Another region of strong convergence is located along the coastline of Texas and eastern Mexico. A major source region lies off the west coast of the Baja peninsula, with maximum values on the order of ~30 cm mo^{-1}. This same region was found to be the strongest summertime source region for North America by Roads et al. (1994). The Gulf of California also shows up as a minor source region, with $E - P$ values in the range of 5–15 cm mo^{-1}.

While the aforementioned source and sink regions seem both physically and quantitatively reasonable, other features of the flux divergence field are more difficult to comprehend. In particular, the strongest source region in our analysis domain, with $E - P$ values greater than 40 cm mo^{-1}, lies over the southern Rio Grande River Valley. This same feature pervades the flux divergence of all eight summers in our data sample. The sign of the divergence may be realistic as monthly precipitation in May and June runs 10%–50% larger than in July and August over northeast Mexico and south Texas (Douglas et al. 1993; NOAA 1982). The greater rainfall in late spring could provide the potential for evaporation to exceed precipitation during the summer. It is interesting to note that prior studies have also found this area to be a source of water vapor during the summer (Rasmusson 1966; Roads et al. 1994). The magnitude of the flux divergence, on the other hand, is very dubious. Comparison of the $\bar{q}\nabla\cdot\mathbf{V}$ and $\mathbf{V}\cdot\nabla\bar{q}$ fields suggests that the large magnitude results primarily from an overestimate of the divergence of the low level wind in the region. It is not clear what factors cause the extreme divergence, but improper adjustment of the low-level wind to the model's distri-

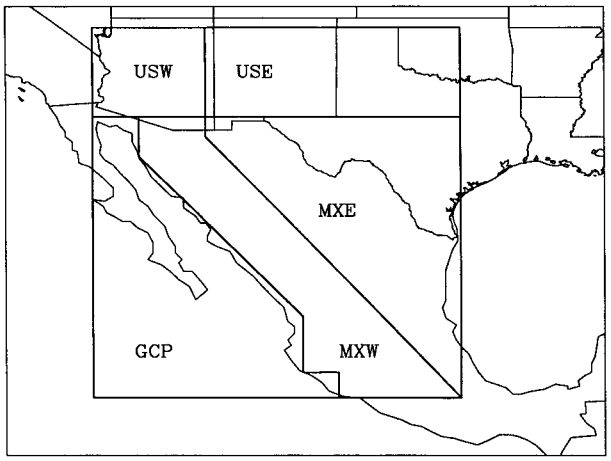

FIG. 10. Geographical areas used in the calculations of the regional water vapor balances and moisture transport across regional boundaries.

bution of terrain and/or use of only surface and mandatory level analyses in the vertical integrations (i.e., much coarser vertical resolution than the original ECMWF sigma-level analyses) are suspected.

Estimates of the spatially averaged rmse (assuming radiosonde accuracy at each grid point) suggest an uncertainty of 0.6 g cm^{-2} mo^{-1}, but the large divergence over the lower Rio Grande valley suggests that much larger errors exist in our analysis. Since surface runoff SR must equal $P - E$ (assuming surface and underground storage are negligible), some limited comparisons can be made with actual streamflow measurements for the southwest United States. Using the streamflow data for the United States of Wallis et al. (1991), we find that $E - P$ is about an order of magnitude too large over the Mogollon Rim, the southeast Texas coast, and most of New Mexico. Streamflow data also indicate a net runoff ($SR > 0$) in the lower Rio Grande valley, implying an atmospheric sink of moisture exists there rather than a major source as depicted by our analysis. Runoff data for Mexico have not been compared, although precipitation data over western Mexico, as presented by Douglas et al. (1993), suggest the distribution of $E - P$ is realistic but ~50% too large. In consideration of these uncertainties, the change in sign of the divergence field is not important if its value is near zero. Consequently the zero contour was omitted in Fig. 9.

On the whole, we believe that our estimates of the atmospheric balance are qualitatively realistic in terms of the sense of sign over most regions, but the mandatory level ECMWF analyses alone, even at a T106 resolution, do not in general yield accurate quantitative estimates of the local balance of water vapor over the entire region.

c. *Regional balance of water vapor and moisture transport across regional boundaries*

The first two parts of this study focused on documenting the water vapor flux and its divergence at the resolution of the T106 ECMWF analyses. Our diagnosis suggests that the mandatory level analyses are not accurate enough to produce physically realistic estimates of highly differentiated quantities such as the flux divergence. For this reason, regionally averaged flux divergences and fluxes across the regional boundaries are calculated with the goal of obtaining a more meaningful depiction of the primary sources and sink regions of water vapor.

Area-average divergences and lateral boundary fluxes (LBFs) were computed for five regions that were selected on the basis of the underlying terrain. These subregions are illustrated in Fig. 10 and were defined as follows: the United States east (USE) and west (USW) of the Continental Divide; Mexico east (MXE) and west (MXW) of the crest of the Mexican Plateau as portrayed by the T106 terrain field; and the Gulf of California–Pacific (GCP). Values for the SFC–700 mb layer are identified by the subscript L for low level, and those for the 700–200-mb layer by the subscript U for upper level.

The area-averaged moisture budgets for the SFC–200-mb column (Fig. 11) indicate that three land regions USW, USE, and MXW are sinks for water vapor while the one ocean region GCP is a source. The flux convergence for MXW, the region of greatest July–August precipitation, is an order of magnitude larger than those for USW and USE. This distribution seems physically plausible. The MXE region, however, is also a source region since it contains the spurious divergences over the lower Rio Grande valley. The sensitivity of the area-average divergences to modest shifts (± one grid point) in their boundaries was tested. We find that the sense of divergence can be sensitive to such shifts with the exception of the MXW sector, which always remains a region of strong convergence.

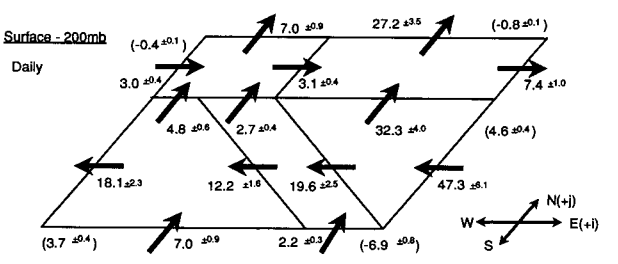

FIG. 11. July–August, regional water vapor balance and horizontal fluxes across regional boundaries for the surface to 200-mb layer. Dark arrows indicate the direction of the net horizontal transport across each face of the volume. Magnitudes are presented as 10^{16} grams $month^{-1}$. Numbers in parenthesis indicate the net flux divergence (positive number) for the adjacent volume. Estimated uncertainties for all quantities are indicated by the ± number following each value.

The LBFs for the SFC–200-mb layer indicate that ~80% of the total water vapor transported into the entire domain comes from over the Gulf of Mexico. All moisture from the Gulf of Mexico initially enters the MXE sector. More than half (~60%) of the moisture that leaves MXE heads northward into USE. The remainder (~40%) crosses the Mexican Plateau and enters the MXW region. Thus, ~90% of the moisture transported into both the USE and MXW regions comes from over the Gulf of Mexico. The majority of the moisture exiting the USE region flows northward into Colorado and Kansas. Most of the water vapor (~80%) that exits the MXW region continues westward into GCP; the remainder enters the USW through southeast Arizona. A comparable amount of moisture flows into the USW from the west, but most moisture entering the USW sector comes from the GCP region.

If the atmosphere above and below 700 mb is examined separately (Fig. 12), a different perspective is obtained. The sense of the LBFs for the SFC–700-mb and the 700–200-mb layers are the same as those for the SFC–200-mb layer with one important exception: the low-level flux is oriented from the GCP_L into the MXW_L. This means that moisture from the Gulf of Mexico that crosses the MXE_L–MXW_L border does not flow through the western boundary of MXW_L. Thus, any moisture flowing into USW_L from the GCP_L sector must be of Pacific origin. The southerly flux across the MXW_L–USW_L border would be a mixture of water vapor from the Gulf of California, the tropical East Pacific and the Gulf of Mexico.

With inward fluxes along three of its four boundaries, strong convergence is forced in the MXW_L sector, which leads to a vigorous upward transport of water vapor into MXW_U. In fact, the vertical flux from the MXW_L is the largest source of moisture for the 700–200-mb layer. In conjunction with the weaker upward fluxes over the other land sectors, vertical transports account for more than ~50% of the water vapor input aloft.

The sensitivity of the boundary fluxes to modest shifts (± one grid point) in the position of the regional boundaries was also examined. We find that the magnitudes of the boundary fluxes typically change by 10%, but their components normal to the boundaries remain the same with the exception of the weak 700–200-mb flux along the western boundary of USW and the 700-mb vertical flux over GCP. The impact of raising the layer interface from 700–600 mb was also examined and found to not affect the sense of the fluxes. Thus, we believe the results concerning the strong boundary fluxes discussed above are qualitatively robust.

6. Discussion and conclusions

In this study, the origins and transport of water vapor into the semi-arid Sonoran Desert region of North America were examined for the July–August monsoon season. Mandatory level analyses produced by ECMWF at a spectral truncation of triangular 106 were used to compute vertically integrated fluxes and flux divergences of water vapor.

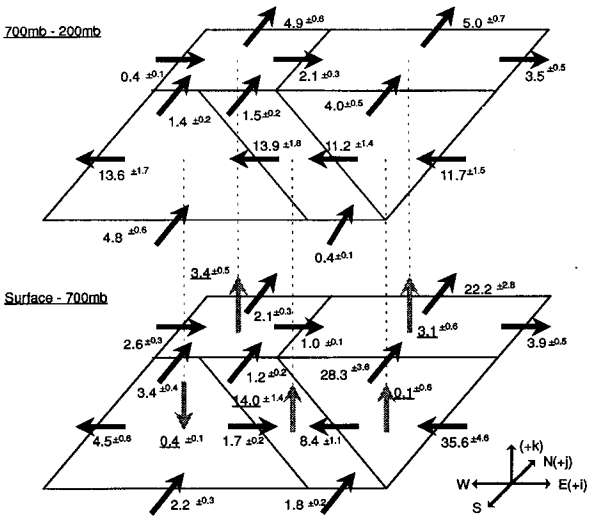

FIG. 12. July–August, horizontal fluxes of water vapor across regional boundaries for the 700–200-mb layer (top) and SFC–700-mb layer (bottom), and vertical fluxes through the 700-mb interface. Dark arrows indicate the direction of the net horizontal transport across each face of the volume; gray arrows denote the direction of net vertical transport across the 700-mb level. Plain (underlined) values represent the (vertical) moisture transport through the 700-mb level. Magnitudes are presented as 10^{16} grams per month. Estimated uncertainties for all quantities are indicated by the ± number following each value.

The T106 ECMWF analyses, interpolated to only the mandatory levels, do not possess sufficient precision to yield accurate estimates of highly differentiated quantities such as the divergence of the vertically integrated flux of water vapor. Perhaps calculation of the water balance using the T106 ECMWF analyses on their original sigma/hybrid layers would remedy the problem of dubious source regions over the North American continent (such as the major source over the lower Rio Grande valley); calculations on sigma levels have proven useful in prior studies that used model output to compute budgets of other atmospheric quantities (e.g., Sardeshmukh and Held 1984; Mullen 1986).

Some insight into the importance of inadequate vertical resolution and analysis biases in the ECMWF system on dubious source regions can be obtained by comparing differences between raw radiosonde data and the ECMWF analyses interpolated to radiosonde sites. While we have not performed a detailed comparison at this time, a cursory examination of differences over Tucson, Arizona, (Table 1) is illuminating. The vector difference between the time-mean, vertically integrated moisture flux based on the radiosonde data at 10-mb

TABLE 1. Comparison over Tucson, Arizona, of vertically integrated (SFC–200 mb) moisture flux based on ECWMF analyses at mandatory levels ($ECMWF_m$), radiosonde data at mandatory levels ($RAOB_m$) and radiosonde data interpolated to every 10 mb ($RAOB_{10}$) prior to vertical integration. ECMWF values at Tucson were obtained by bilinear interpolation from the analysis grid. The comparison period is for the eight July–August seasons 1985–1992. The first row gives the flux vector magnitude (gm $cm^{-1}s^{-1}$) and meteorological direction; the second row gives the vector error (g $cm^{-1}s^{-1}$) between the indicated value and the 10-mb radiosonde value, which is assumed to be the best estimate of "truth."

	$RAOB_{10}$	$RAOB_m$	$ECMWF_m$
Flux	223@216°	209@220°	223@186°
Error		21@351°	116@111°

increments (assumed to be "truth") and on the mandatory levels only is relatively modest, being less than 10%. However, its impact on the divergence would be much larger if such differences project even slightly onto the irrotational modes. This suggests that the use of only mandatory data per se could lead to erroneous flux divergences. The vector differences between the mandatory level ECMWF analyses and both the 10-mb and mandatory radiosonde data are much larger (~50%), along with any probable degradation of the flux divergence. While we have not yet examined whether such large discrepancies exist at other radiosonde sites in the Sonoran region, it is clear that the ECMWF analysis system, for reasons unknown to us at this time, can contain biases as large as 50% in the time-mean vector flux of vertically averaged water vapor. In view of the above results for Tucson, we find it encouraging that the regional distribution of the moisture flux divergence based on the T106 ECMWF mandatory analyses seems physically reasonable over most of the study domain. For this reason, we still believe that the T106 mandatory level analyses, for the most part, provide a faithful *qualitative* portrait of *large-scale* features of the vertically integrated, horizontal transport of water vapor.

As a way to summarize what we believe are the most robust results of this study, we offer the schematic diagram of Fig. 13. The figure portrays the primary streams of water vapor by the time-mean circulation for July–August as depicted by the T106 ECMWF analyses. These results can be summarized as follows:

- The transport of water vapor by the time-mean circulation dominates that due to the transient eddies.
- Most water vapor enters the Sonoran region at low levels (below 700 mb). This moisture comes primarily from over the northern Gulf of California, but limited amounts from the Gulf of Mexico flow over the Sonoran Gap into the eastern Sonoran Desert. The time-mean flow is unable to transport water vapor directly from the southern Gulf of California and/or tropical East Pacific to the Sonoran Desert at low levels.
- Most of the upper-level (above 700 mb) moisture over the Sonoran Desert appears to come from over the Gulf of Mexico, circulating around the southern and western quadrants of the subtropical ridge.
- Onshore, low-level flow from the southern Gulf of California and the tropical East Pacific produces a convergence of water vapor that helps fuel the persistent convection along the west slopes of the Sierra Madre Occidental. The convection injects a large amount of water vapor into the upper levels. Once aloft, this tropical moisture may reach the western Sonoran Desert after subsequent northwestward transport by the mean flow.

While our results support the notion that the northern Gulf of California is a major source of low-level moisture for the Sonoran Desert, evidence exists that the impact of the Gulf on the regional climate is not properly resolved by the T106 ECMWF analyses. The land–sea mask for the ECMWF analyses (Fig. 14) reveals that the northern Gulf of California is represented by two inland seas at a T106 truncation. The ECMWF terrain field (Fig. 14) indicates that mountains of the Baja peninsula are also poorly resolved, especially over northern most Baja California where the actual elevations along the crest run higher than 1000 m but the analysis system produces heights around 500 m. The lower barrier in the T106 ECMWF analysis system could prevent the blocking of the low-level northwesterlies to the west of northern Baja California and lead to an excessive penetration of low-level westerly momentum across the peninsula into the northern Gulf of California. This could help explain surface southwesterlies in the T106 ECMWF analyses over a region where observations from special field programs (Badan-Dangon et al. 1991; Douglas et al. 1993) indicate prevailing S–SSE winds.

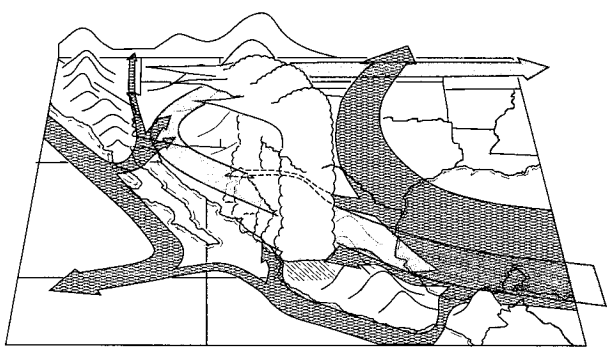

FIG. 13. Schematic of the most robust features of the 3D transport of moisture as inferred from the T106 ECMWF analyses. The cross-hatched arrows denote the primary streams of low-level (SFC–700 mb) moisture; the shaded arrow denotes the primary stream of the moisture aloft (700–200 mb). Width of the arrows is proportional to the magnitude of the horizontal moisture flux. Cumulonimbus clouds denote the region of strongest upward flux of water vapor and maximum precipitation.

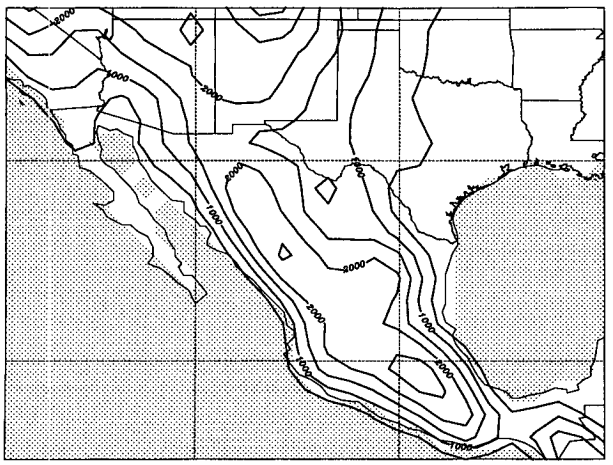

FIG. 14. Terrain heights (contour interval 500 m, with zero contour omitted) and the land–sea mask (hatching indicates ocean areas) for the T106 ECMWF analyses.

The inadequate resolution of the local geography at a T106 truncation has important consequences for future studies that examine the North American monsoon. For example, current reanalysis efforts will not address the situation because they employ horizontal resolutions of T106 or coarser (e.g., Kalnay and Jenne 1991; Gibson et al. 1994; Janowiak et al. 1994; Kistler et al. 1994). Despite the higher vertical resolution of the reanalysis products, which should improve the accuracy of estimates of the vertically integrated moisture flux and its divergence, we believe that diagnostic studies based on the reanalysis output may provide little additional insight into the impact of the Gulf of California and regional-scale circulations on the monsoon over that already obtainable from the current T106 ECMWF analyses because of inadequate horizontal resolution.

Clearly resolutions finer than T106 are required before the regional-scale circulations associated with the North American monsoon can be understood. We believe that simulations with regional climate models (RCMs), employing horizontal and vertical resolutions higher than the T106 ECMWF mandatory level analyses, may offer the most economical means to achieve this goal. However, the ability of RCMs to simulate faithfully the monsoon has not been firmly established. Pioneering simulations (e.g., Giorgi 1991; Giorgi et al. 1994) of the Sonoran region missed the most important features of the monsoon such as maximum summer precipitation being over western Mexico. Using four-dimensional data assimilation to ingest special field observations, Stensrud et al. (1995) showed that 24-h simulations with a suitably constructed, properly initialized mesoscale model can capture many of the salient features of the monsoon, such as low-level mean flow up the Gulf of California and the axis of maximum precipitation along the western foothills of the Sierra Madre Occidental. While the results of Stensrud et al. (1995) are encouraging, they did not examine whether simulations would be nearly as accurate if the special observations were excluded or if the integrations were extended beyond 24 h. Ultimately, long-term observations in the immediate vicinity of the Gulf of California, similar in scope to those analyzed by Badan-Dangon et al. (1991) and Douglas et al. (1993) for single summers, will be needed to validate climate models, to use for mesoscale data assimilations, and to determine the true role of the Gulf of California.

Even though our results indicate that the time-mean circulation dominates the transport of water vapor, we believe that the role of transience needs to be thoroughly examined. As previously noted, the temporal variability in summertime rainfall over the Sonoran region attests to the importance of transience in modulating precipitation (Bryson and Lowry 1955; Carleton 1986; Watson et al. 1994). Research is under way, using the T106 ECMWF analyses, that contrasts the larger-scale circulation and moisture transport during "bursts" and "breaks" in the monsoonal rainfall over the Sonoran Desert. Results will be reported in due course.

Acknowledgments. The authors thank the two anonymous reviewers for their insightful comments, especially their suggestion to examine differences between the ECMWF analyses and radiosonde data more closely. This paper is based on the doctoral dissertation of the first author (JTS). This work was supported by NASA Grant NAG-51642. The second author (SLM) was also partially supported by NSF Grant ATM-9319411. Prof. J. Zehnder aided with the derivation of the appendix.

APPENDIX

Derivation of the Time-Mean Balance of Water Vapor

The water vapor balance per unit mass for a parcel of air as given by Rasmusson (1977) is

$$\frac{dq}{dt} = \frac{\partial q}{\partial t} + \mathbf{V}\cdot\nabla q + \omega\frac{\partial q}{\partial p} = e - c + g\frac{\partial D}{\partial p}, \quad \text{(A1)}$$

where

- g gravitational acceleration,
- t time,
- p pressure,
- $\mathbf{V}$ horizontal velocity vector,
- ω pressure vertical velocity,
- e evaporation per unit mass for an air parcel,
- c condensation rate per unit mass for an air parcel,
- q specific humidity, and
- D vertical diffusion rate per unit area of atmospheric water vapor.

With the aid of the mass continuity equation, (A1) can be transformed into

$$e - c + g\frac{\partial D}{\partial p} = \frac{\partial q}{\partial t} + \nabla\cdot q\mathbf{V} + \frac{\partial \omega q}{\partial p}, \quad \text{(A2)}$$

which is the water vapor balance equation for a particular isobaric level. The total transport within a column of air is obtained by integrating with respect to pressure from the top of the atmosphere p_{top} to the surface of the earth p_{sfc}, which gives

$$\int_{p_{\text{top}}}^{p_{\text{sfc}}} (e - c)\frac{dp}{g} + \int_{p_{\text{top}}}^{p_{\text{sfc}}} g\frac{\partial D}{\partial p}\frac{dp}{g} = \int_{p_{\text{top}}}^{p_{\text{sfc}}} \frac{\partial q}{\partial t}\frac{dp}{g} + \int_{p_{\text{top}}}^{p_{\text{sfc}}} \nabla\cdot q\mathbf{V}\frac{dp}{g} + \int_{p_{\text{top}}}^{p_{\text{sfc}}} \frac{\partial \omega q}{\partial p}\frac{dp}{g}. \quad \text{(A3)}$$

At this point Leibnitz' rule (e.g., Hildebrand 1962, 360) is employed, which states that given a function

$$F(x, y) = \int_{A(x)}^{B(x)} f(x, y)dy$$

the partial derivative of F with respect to x has the form

$$\frac{\partial F(x, y)}{\partial x} = \int_{A(x)}^{B(x)} \frac{\partial f(x, y)}{\partial x}dy + \left[f(x, B)\frac{\partial B}{\partial x}\right] - \left[f(x, A)\frac{\partial A}{\partial x}\right].$$

Applying Leibnitz' rule to the first two terms on the right-hand side of (A3), we get

$$\int_{p_{\text{top}}}^{p_{\text{sfc}}} \frac{\partial q}{\partial t}\frac{dp}{g} + \int_{p_{\text{top}}}^{p_{\text{sfc}}} \nabla\cdot q\mathbf{V}\frac{dp}{g} = \frac{\partial W}{\partial t} + \nabla\cdot\langle q\mathbf{V}\rangle - \frac{q_{\text{sfc}}}{g}\left[\frac{\partial p_{\text{sfc}}}{\partial t} + \mathbf{V}_{\text{sfc}}\cdot\nabla p_{\text{sfc}}\right] + \frac{q_{\text{top}}}{g}\left[\frac{\partial p_{\text{top}}}{\partial t} + \mathbf{V}_{\text{top}}\cdot\nabla p_{\text{top}}\right],$$

where

$$\langle(\quad)\rangle = \int_{p_{\text{top}}}^{p_{\text{sfc}}} (\quad)\frac{dp}{g},$$

$W = \langle q\rangle$ is the precipitable water, and $\mathbf{Q} = \langle q\mathbf{V}\rangle$ is the vertically integrated water vapor flux. The last term in brackets is zero since p_{top} is fixed at 200 mb. The first term in brackets is ω_{sfc} since

$$\omega_{\text{sfc}} = \frac{\partial p_{\text{sfc}}}{\partial t} + \mathbf{V}_{\text{sfc}}\cdot\nabla p_{\text{sfc}}$$

at $p = p_{\text{sfc}}$ (e.g., Panofsky 1946; Haltiner and Williams 1980; Trenberth 1991). After simplification, we finally obtain

$$\int_{p_{\text{top}}}^{p_{\text{sfc}}} \frac{\partial q}{\partial t}\frac{dp}{g} + \int_{p_{\text{top}}}^{p_{\text{sfc}}} \nabla\cdot q\mathbf{V}\frac{dp}{g} = \frac{\partial \mathrm{W}}{\partial \mathrm{t}} + \nabla\cdot\mathbf{Q} - \frac{q_{\text{sfc}}\omega_{\text{sfc}}}{g}. \quad \text{(A4)}$$

Substitution of (A4) into (A3) and integration of all terms results in

$$-P + D(p_{\text{sfc}}) - D(p_{\text{top}}) = \frac{\partial W}{\partial t} + \nabla\cdot\mathbf{Q} - \frac{q_{\text{top}}\omega_{\text{top}}}{g}, \quad \text{(A5)}$$

where it is generally assumed (Rasmusson 1977) that

$$\int_{p_{\text{top}}}^{p_{\text{sfc}}} (e - c)\frac{dp}{g} = -P.$$

From (A5) it is clear that $\omega_{\text{sfc}}q_{\text{sfc}}/g$ produced by vertically integrating the vertical flux divergence terms cancels the $\omega_{\text{sfc}}q_{\text{sfc}}/g$ resulting from application of Leibnitz's rule. Historically, this term has been treated in one of two ways: most commonly it is set to zero by assuming ω_{sfc} is zero (Palmén 1967; Rasmusson 1967, 1968, 1977)—that is, a "flat earth" assumption; less frequently it is used to represent evapotranspiration at scales too small to resolve (Peixoto 1973).

Several more terms can be eliminated following the integration of (A5). Here, $\omega_{\text{top}}q_{\text{top}}/g$ becomes negligible since $q_{\text{top}} \approx 0$. Similarly, the vertical diffusion at the top of the atmosphere $D(p_{\text{top}})$ can be neglected. This leaves

$$E - P = \frac{\partial W}{\partial t} + \nabla\cdot\mathbf{Q}, \quad \text{(A6)}$$

where

$$\lim_{p\to p_{\text{sfc}}} D(p) = E.$$

Equation (A6) is the general water balance equation of the atmosphere with horizontal diffusion and the contributions from liquid and solid phases neglected.

REFERENCES

Badan-Dangon, A., C. E. Dorman, M. A. Merrifield, and C. D. Winant, 1991: The lower atmosphere over the Gulf of California. *J. Geophys. Res.*, **96,** 16 877–16 896.

Benton, G. S., and M. A. Estoque, 1954: Water-vapor transfer over the North American continent. *J. Meteor.*, **11,** 462–477.

Brenner, I. S., 1974: A surge of maritime tropical air—Gulf of California to the southwestern United States. *Mon. Wea. Rev.*, **102,** 375–389.

Bryson, R. A., and W. P. Lowry, 1955: The synoptic climatology of the Arizona summer precipitation singularity. *Bull. Amer. Meteor. Soc.*, **36,** 329–339.

Carleton, A. M., 1985: Synoptic and satellite aspects of the southwestern U.S. summer "monsoon." *J. Climatol.*, **5,** 389–402.

——, 1986: Synoptic-dynamic character of "bursts" and "breaks" in the south-west U.U. summer precipitation singularity. *J. Climatol.*, **6,** 605–623.

——, D. A. Carpenter, and P. J. Weser, 1990: Mechanisms of interannual variability of the southwest United States summer rainfall maximum. *J. Climate,* **3,** 999–1015.

Douglas, M. W., R. A. Maddox, K. Howard, and S. Reyes, 1993: The Mexican monsoon. *J. Climate,* **6,** 1665–1677.

Gibson, J. K., A. Hernandez, P. Kallberg, A. Nomura, E. Serrano, and S. Uppala, 1994: The ECMWF re-analysis (ERA) project—Plans and current status. Preprints, *10th Conf. on Numerical Weather Prediction,* Portland, OR, Amer. Meteor. Soc., 288–291.

Giorgi, F., 1991: Sensitivity of simulated summertime precipitation over the western United States to different physics parameterizations. *Mon. Wea. Rev.,* **119,** 2870–2888.

——, C. S. Brodeur, and G. T. Bates, 1994: Regional climate change scenarios over the United States produced with a nested regional climate model. *J. Climate,* **7,** 375–399.

Hagemeyer, B. C., 1991: A lower tropospheric climatology for March through September: Some implications for thunderstorm forecasting. *Wea. Forecasting,* **6,** 254–270.

Hales, J. E., Jr., 1972: Surges of maritime tropical air northward over the Gulf of California. *Mon. Wea. Rev.,* **100,** 298–306.

——, 1974: Southwestern United States summer monsoon source—Gulf of Mexico or Pacific Ocean? *J. Appl. Meteor.,* **13,** 331–342.

Haltiner, G. J., and R. T. Williams, 1980: *Numerical Prediction and Dynamic Meteorology.* John Wiley and Sons, 477 pp.

Hildebrand, F. B., 1962: *Advanced Calculus for Applications.* Prentice-Hall, 646 pp.

Janowiak, J. E., W. Ebisuzaki, M. Chelliah, S. Saha, R. Kistler, M. Kanamitsu, and G. White, 1994: Reanalysis archives. Preprints, *10th Conf. on Numerical Weather Prediction,* Portland, OR, Amer. Meteor. Soc., 286–287.

Jurwitz, L., 1953: Arizona's two season rainfall pattern. *Weatherwise,* **6,** 96–99.

Kalnay, E., and R. Jenne, 1991: Summary of the NMC/NCAR reanalysis workshop of April 1991. *Bull. Amer. Meteor. Soc.,* **72,** 1897–1904.

Kistler, R., M. Kanamitsu, and E. Kalnay, 1994: Overview of the NMC/NCAR reanalysis system. Preprints, *10th Conf. on Numerical Weather Prediction,* Portland, OR, Amer. Meteor. Soc., 279–280.

Mullen, S. L., 1986: The local balances of vorticity and heat for blocking anticyclones in a spectral general circulation model. *J. Atmos. Sci.,* **43,** 1406–1441.

Negri, A. J., R. F. Adler, E. J. Nelkin, and G. J. Huffman, 1994: Regional rainfall climatologies derived from special sensor microwave imager (SSM/I) data. *Bull. Amer. Meteor. Soc.,* **75,** 1165–1182.

NOAA, 1982: Climatography of the United States No. 81 (by state), monthly normals of temperature, precipitation, heating and cooling degree days 1951–1980, Texas. National Oceanic and Atmospheric Administration, Environmental Data and Information Service, National Climatic Center, Asheville, N.C.

Oort, A. H., 1983: Global atmospheric circulation statistics 1958–1973. NOAA Professional Paper 14, 180 pp.

Palmén, E., 1963: Computation of evaporation over the Baltic Sea from the flux of water vapor in the atmosphere. *Int. Assoc. Sci. Hydrol.,* **62,** 244–252.

——, 1967: Evaluation of atmospheric moisture transport for hydrological purposes. WMO Publ. No. 1, 63 pp.

Panofsky, H. A., 1946: Methods of computing vertical motion in the atmosphere. *J. Meteor.,* **3,** 45–49.

Peixoto, J. P., 1973: *Atmospheric Vapour Flux Computations for Hydrological Purposes.* WMO Publ. No. 357, 83 pp.

——, and A. H. Oort, 1983: The atmospheric branch of the hydrological cycle and climate. *Variations in the Global Water Budget,* A. Street-Perrott, M. Beran, and R. Ratcliff, Eds., D. Reidel Publishing, 518 pp.

——, and ——, 1992: *Physics of Climate.* American Institute of Physics, 520 pp.

Rasmusson, E. M., 1966: Atmospheric water vapor transport and the hydrology of North America. Report No. A-1, Planetary Circulations Project, Massachusetts Institute of Technology, 170 pp.

——, 1967: Atmospheric water vapor transport and water balance of North America. Part I: Characteristics of the water vapor flux field. *Mon. Wea. Rev.,* **95,** 403–426.

——, 1968: Atmospheric water vapor transport and water balance of North America. Part II: Large scale water balance investigations. *Mon. Wea. Rev.,* **96,** 720–734.

——, 1977: *Hydrological Application of Atmospheric Vapour-Flux Analyses.* WMO Publ. No. 476., 50 pp.

Reed, T. R., 1933: The North American high-level anticyclone. *Mon. Wea. Rev.,* **61,** 321–325.

Reitan, C. H., 1957: The role of precipitable water vapor in Arizona's summer rains. Tech. Rep. on the Meteorology and Climatology of Arid Regions 2, Institute of Atmospheric Physics, The University of Arizona, Tucson, Arizona.

Reyes, S., and D. L. Cadet, 1986: Atmospheric water vapor and surface flow patterns over the tropical Americas during May–August 1979. *Mon. Wea. Rev.,* **114,** 582–593.

——, and ——, 1988: The southwest branch of the North American monsoon during summer 1979. *Mon. Wea. Rev.,* **116,** 1175–1187.

Roads, J. O., S. Chen, A. K. Guetter, and K. P. Georgakakos, 1994: Large-scale aspect of the United States hydrologic cycle. *Bull. Amer. Meteor. Soc.,* **75,** 1589–1610.

Rosen, D. R., D. A. Salstein, and J. P. Peixoto, 1979: Variability in the annual fields of large scale atmospheric water vapor transport. *Mon. Wea. Rev.,* **107,** 26–37.

Sardeshmukh, P. D., and I. M. Held, 1984: The vorticity balance in the tropical upper troposphere of a general circulation model. *J. Atmos. Sci.,* **41,** 768–778.

Sellers, W. D., and R. H. Hill, 1974: *Arizona Climate, 1931–1972.* The University of Arizona Press, 616 pp.

Starr, V. P., and J. P. Peixoto, 1958: On the global balance of water vapor and the hydrology of deserts. *Tellus,* **10,** 188–194.

——, ——, and A. R. Crisi, 1965: Hemispheric water balance for IGY. *Tellus,* **17,** 463–472.

Stensrud, D. J., R. L. Gall, S. L. Mullen, and K. W. Howard, 1995: Model climatology of the Mexican monsoon. *J. Climate,* **8,** 1775–1794.

Trenberth, K. E., 1991: Climate diagnostics from global analyses: Conservation of mass in ECMWF analyses. *J. Climate,* **4,** 707–722.

——, and J. G. Olson, 1988: An evaluation and intercomparison of global analyses from the National Meteorological Center and the European Centre for Medium-Range Weather Forecasts. *Bull. Amer. Meteor. Soc.,* **69,** 1047–1057.

Wallis, J. R., D. P. Lettenmaier, and E. F. Wood, 1991: *A Daily Hydroclimatological Data Set for the Continental United States.* NDGC, CD-ROM. [Available from National Geophysical Data Center, NOAA E/GC1, 325 Broadway, Boulder, CO 80303.]

Watson, A. I., R. E. Lopez, and R. L. Holle, 1994: Diurnal cloud-to-ground lightning patterns in Arizona during the southwest monsoon. *Mon. Wea. Rev.,* **122,** 1716–1725.